The Astrophysical Journal, 683:346–356, 2008 August 10

MODELS FOR LOW-MASS X-RAY BINARIES IN THE ELLIPTICAL GALAXIES NGC 3379 AND NGC 4278: COMPARISON WITH OBSERVATIONS

T. Fragos,[1] V. Kalogera,[1] K. Belczynski,[2] G. Fabbiano,[3] D.-W. Kim,[3] N. J. Brassington,[3] L. Angelini,[4] R. L. Davies,[5] J. S. Gallagher,[6] A. R. King,[7] S. Pellegrini,[8] G. Trinchieri,[9] S. E. Zepf,[10] A. Kundu,[10] and A. Zezas[3]

Received 2007 December 21; accepted 2008 March 6

ABSTRACT

We present theoretical models for the formation and evolution of populations of low-mass X-ray binaries (LMXBs) in the two elliptical galaxies NGC 3379 and NGC 4278. The models are calculated with the recently updated StarTrack code, assuming only a primordial galactic field LMXB population. StarTrack is an advanced population synthesis code that has been tested and calibrated using detailed binary star calculations and incorporates all the important physical processes of binary evolution. The simulations are targeted to modeling and understanding the origin of the X-ray luminosity functions (XLFs) of point sources in these galaxies. For the first time we explore the population XLF in luminosities below 10^{37} ergs s^{-1}, as probed by the most recent observational results. We consider models for the formation and evolution of LMXBs in galactic fields with different CE efficiencies, stellar wind prescriptions, magnetic braking laws, and IMFs. We identify models that produce XLFs consistent with the observations both in shape and absolute normalization, suggesting that a primordial galactic field LMXB population can make a significant contribution to the total population of an elliptical galaxy. We also find that the treatment of the outburst luminosity of transient systems remains a crucial factor for the determination of the XLF, since the modeled populations are dominated by transient X-ray systems.

Subject headings: binaries: close — galaxies: elliptical and lenticular, cD — stars: evolution — X-rays: binaries

Online material: additional figures, machine-readable table

1. INTRODUCTION

A low mass X-ray binary (LMXB) is a Roche lobe–overflowing, mass-transferring binary system with a compact object accretor, either a black hole (BH) or a neutron star (NS), and a low-mass ($\gtrsim 1\ M_{\odot}$) donor. Since the late 1980s it has been suggested that LMXBs should exist in early-type galaxies (E and S0) and that they might even dominate the X-ray emission (Trinchieri & Fabbiano 1985; Fabbiano 1989; Kim et al. 1992). The stellar populations in these galaxies are typically old and homogeneous. Massive stars have already evolved to compact objects, and LMXBs are probably the only sources with X-ray luminosities above 10^{36} ergs s^{-1}.

Uncontroversial detection of LMXBs in early-type galaxies became possible only this last decade with *Chandra's* increased angular resolution (Fabbiano 2006; Sarazin et al. 2000). The spectra of individual X-ray sources are consistent with those expected from LMXB models and the LMXBs observed in the Milky Way and M31 (Humphrey & Buote 2006; Irwin et al. 2003). For many galaxies observed with *Chandra*, the XLFs have been derived, and they can usually be fitted with a single or a broken power law. The detections limit for these surveys is usually a few times 10^{37} ergs s^{-1}. Kim & Fabbiano (2004) derived XLFs for 14 early-type galaxies, and they included completeness corrections. Each XLF is well fitted with a single power law with cumulative slope between -0.8 and -1.2. The composite XLF of these galaxies, however, is not consistent with a single power law. There is a prominent break at $(5 \pm 1.6) \times 10^{38}$ ergs s^{-1}, close to the Eddington luminosity ($L_{\rm Edd}$) of a helium-accreting NS-LMXB. This break might be hidden in the individual XLFs due to poor statistics (see also Sarazin et al. 2000; Kundu et al. 2002; Jordán et al. 2004; Gilfanov 2004). Other recent studies by Jeltema et al. (2003), Sivakoff et al. (2003), and Jordán et al. (2004) suggested a break of the XLF at a higher luminosity ($\sim 10^{39}$ ergs^{-1}). The exact position and the nature of these breaks are still somewhat controversial, as the correct interpretation of the observed XLFs relies significantly on the proper completeness correction when looking at luminosities close to the detection limit and small number statistics at the high end of the XLF.

Recent *Chandra* observations (Kim et al. 2006a) have yielded the first low-luminosity XLFs of LMXBs for two typical old elliptical galaxies, NGC 3379 and NGC 4278. The detection limit (corresponding to the lowest luminosity source that is detected) in these observations is $\sim 3 \times 10^{36}$ ergs s^{-1}, which is about an order of magnitude lower than in most previous surveys of early-type galaxies. The observed XLFs of the two ellipticals extend only up to 6×10^{38} ergs s^{-1} and are well represented by a single power law with a slope (in a differential form) of 1.9 ± 0.1.

[1] Department of Physics and Astronomy, Northwestern University, 2145 Sheridan Road, Evanston, IL 60208; tassosfragos@northwestern.edu, vicky@northwestern.edu.
[2] Department of Astronomy, New Mexico State University, 1320 Frenger Mall, Las Cruces, NM 88003; kbelczyn@nmsu.edu.
[3] Harvard-Smithsonian Center for Astrophysics, 60 Garden Street, Cambridge, MA 02138; gfabbiano@cfa.harvard.edu, kim@cfa.harvard.edu, nbrassington@head.cfa.harvard.edu, azezas@cfa.harvard.edu.
[4] Laboratory for High Energy Astrophysics, NASA Goddard Space Flight Center, Code 660, Greenbelt, MD 20771; angelini@davide.gsfc.nasa.gov.
[5] Denys Wilkinson Building, University of Oxford, Keble Road, Oxford OX1 3RH, UK; rld@astro.ox.ac.uk.
[6] Astronomy Department, University of Wisconsin, 475 North Charter Street, Madison, WI 53706; jsg@astro.wisc.edu.
[7] University of Leicester, Leicester LE1 7RH, UK; ark@star.le.ac.uk.
[8] Dipartimento di Astronomia, Università di Bologna, via Ranzani 1, 40127 Bologna, Italy; silvia.pellegrini@unibo.it.
[9] INAF–Observatorio Astronomico di Brera, via Brera 28, 20121 Milan, Italy; ginevra.trinchieri@brera.inaf.it.
[10] Department of Physics and Astronomy, Michigan State University, East Lansing, MI 48824-2320; zepf@pa.msu.edu.

When *Chandra* observations are compared with optical images from *Hubble* or other ground-based telescopes, it is generally found that a significant fraction of the LMXBs are inside globular clusters (GCs). On average 4%–5% of the GCs in a given galaxy are associated with a LMXB (with $L_{\rm x} > \sim 10^{37}$ ergs s^{-1}), while the fraction of LMXBs located in GCs varies from 10% to 70% depending on the type of the galaxy and its GC specific frequency. At present the origin and the properties of these systems, both in GCs and the field, are not yet well understood. It has been noted that XLFs at high luminosities for each subgroup (GCs and field) do not reveal any differences within the statistics of the samples considered (Fabbiano 2006; Kim et al. 2006b; Kundu et al. 2007; Jordán et al. 2004; Sarazin et al. 2003). However, in more recent studies, Fabbiano et al. (2007) and Voss & Gilfanov (2007) independently found that the two XLFs (GCs and field sources) show significant differences at low luminosities (below 10^{37} ergs s^{-1}), pointing to a different LMXB formation mechanism in GCs.

The natural question that arises is whether (1) all LMXBs were formed in GCs through dynamical interactions and some eventually escaped or some GCs dissolved in the field, or (2) field LMXBs were born in situ through binary evolution of primordial binaries. The formation rates associated with these two possibilities are not understood well enough to give accurate predictions and are based on the relative numbers in the samples. Juett (2005) has shown that the observed relationship between the fraction of LMXBs found in GCs and the GC-specific frequency in early-type galaxies is consistent with the galactic field LMXB population being formed in situ. Similarly, Irwin (2005) compared the summed X-ray luminosity of the LMXBs to the number of GCs in a galaxy; in the case of all LMXBs having formed exclusively in GCs, the two should be directly proportional regardless of where the LMXBs currently reside. Instead, he found that the proportionality includes an additive offset, implying the existence of a LMXB population unrelated to GCs.

In the past, semianalytical theoretical models have been introduced for the study of the LMXB population in early galaxies. White & Ghosh (1998) studied the connection between the star formation rates of normal galaxies, i.e., galaxies without an active nucleus, and the formation rate of LMXBs and millisecond pulsars, assuming that all LMXBs are formed from primordial binaries. Considering a time-dependent star formation rate, they showed that the general relativity timescales relevant to the evolution of primordial binaries to LMXBs and to millisecond pulsars lead to a significant time delay of the peak in the formation rate of these populations after the peak in the star formation rate. In a follow-up work Ghosh & White (2001), using several updated star formation rate models, calculated the evolution of the X-ray luminosity of galaxies. They found that different star formation models lead to very different X-ray luminosity profiles, so the observed X-ray profiles can be used as probes of the star formation history. Finally, they compared their models with the first *Chandra* deep imaging observations and concluded that these first results were consistent with current star formation models. Piro & Bildsten (2002) argued that the majority of LMXBs in the field of elliptical galaxies have red giant donors feeding a thermally unstable disk and that they stay in this transient phase for at least 75% of their life. The very luminous X-ray sources ($L_{\rm x} > 10^{39}$ ergs s^{-1}) detected in *Chandra* surveys have been suggested to be X-ray binaries with highly super-Eddington mass inflow near the accreting component. In elliptical galaxies these objects have been suggested by King (2002) to be microquasar-like, as these galaxies contain no high-mass X-ray binaries (King 2002). More recently, Ivanova & Kalogera (2006) also argued that this bright end of the XLF is most likely dominated by transient LMXBs with BH accretors during outburst and that it can be used to derive constraints on the BH mass function in LMXBs; they also showed that the standard assumption of a constant transient duty cycle (DC) across the whole population seems to be inconsistent with current observations.

Semianalytical population synthesis (PS) models of LMXBs have also been constructed for late-type galaxies. Wu (2001) created a simple birth-death model, in which the lifetimes of the binaries are inversely proportional to their X-ray luminosity, and calculated the XLFs of spiral galaxies. His models reproduce certain features, such as the luminosity break in the observed XLFs of spiral galaxies. The position of this break depends on the star formation history of the galaxy, and Wu suggested that it can be used as a probe of the galaxy's merger history. In addition, the presence of faint primordial X-ray binaries in an old galactic component is addressed, predicting for the first time that this population of X-ray binaries should be observable in old galaxies such as the two ellipticals NGC 3379 and NGC 4278.

The formation of LMXBs in GCs via dynamical interactions is less well studied, since apart from the binary stellar evolution, one has to also take into account the complex cluster dynamics. Bildsten & Deloye (2004) considered a semianalytical model for accretion from degenerate donors onto NSs in ultracompact binaries and showed that binaries with orbital periods of 8–10 minutes and He or C/O white dwarf (WD) donors of 0.06–0.08 $M_{\odot}$ naturally provide the primary slope (-0.8 for cumulative form) typically derived from XLFs of elliptical galaxies. Ultracompact systems are predicted to form in the dense GC environment and have relatively short persistent lifetimes ($<3 \times 10^6$ yr), but they form continuously through dynamical interactions. Ivanova et al. (2008) presented PS studies of compact binaries containing NSs in dense GCs. They used StarTrack as their PS modeling tool in addition to a simplified treatment for the dynamical interactions. Their models produced a mixed population of LMXBs, with red giant and MS donors, and ultracompact X-ray binaries; relative formation rates can be comparable, but the different subpopulations have very different lifetimes.

In this paper we use advanced PS simulations to investigate the plausibility of an important contribution being made to the XLFs of these two galaxies by a primordial galactic field LMXB population. In § 2 we describe briefly the physics included in our PS code and explain in detail the way we are constructing the modeled XLFs, as well as the treatment of transient LMXBs. We discuss the results of our simulations in § 3: the modeled XLFs from different models, a statistical comparison with the observed XLFs of the elliptical galaxies NGC 3379 and NGC 4278, and an analysis of the dependence of the modeled XLF properties on the PS parameters. Finally, in § 4 we discuss the implication of our findings and the caveats entailed by our methods.

2. LMXB POPULATION MODELS

For the models presented in this study we focus on LMXBs formed in the galactic field as products of the evolution of isolated primordial binaries. The standard formation channel (Bhattacharya & van den Heuvel 1991; Tauris & van den Heuvel 2006) involves a primordial binary system with a large mass ratio; the more massive star evolves quickly to the giant branch and the system goes into a common envelope (CE) phase. During this phase, the less massive star, which is still dense and unevolved, orbits inside the envelope of the primary and is assumed to remain intact. The orbit of the system changes dramatically, however, as orbital energy is lost due to friction between the unevolved star and the envelope of the giant. Part of the lost orbital energy is used to

TABLE 1
Galaxy Properties

Parameter	NGC 3379	NGC 4278	References
Distance (Mpc)	10.57	16.07	Tonry et al. (2001)
Age (Gyr)	9.3	10.7	Terlevich & Forbes (2002)
Metallicity ([Fe/H])	0.16	0.14	Terlevich & Forbes (2002)
Mass ($M_{\odot}$)	8.6×10^{10}	9.4×10^{10}	Cappellari et al. (2006)
GC specific frequency	1.2	6.9	Ashman & Zepf (1998)

expel the envelope of the giant star. The fraction of the lost orbital energy that is used to heat up the envelope of the giant star and finally expel it defines the CE efficiency factor $\alpha_{\rm CE}$. The CE phase results in a binary system with an unevolved low-mass main-sequence (MS) star orbiting around the core of the massive star in a tighter orbit. The massive core soon reaches core collapse to form a compact object, either a NS or a BH, and the binary orbit is altered due to mass loss and possible supernova kicks. If the binary does not get disrupted or merge in any of the stages described above, angular momentum–loss mechanisms, such as magnetic braking, tides and gravitational wave radiation, will further shrink the orbit and the low-mass companion may evolve off the MS. The companion star eventually overflows its Roche lobe, transferring mass onto the compact object and initiating the system's X-ray phase. An alternative formation channel for NS-LMXBs is through the accretion-induced collapse of a WD accretor into a NS. These systems have generally very low X-ray luminosity and do not affect the LMXB population in the luminosity range that we are interested in this paper.

2.1. *Synthesis Code: StarTrack*

We perform the simulations presented here with StarTrack (Belczynski et al. 2002, 2008), a advanced PS code that has been tested and calibrated using detailed mass transfer calculations and observations of binary populations, and incorporates all the important physical processes of binary evolution: (1) The evolution of single stars and noninteracting binary components, from ZAMS to remnant formation, is followed with analytic formulae (Hurley et al. 2000). Various wind mass-loss rates that vary with the stellar evolutionary stage are incorporated into the code, and their effect on stellar evolution is taken into account. (2) Throughout the course of binary evolution, the changes in all the orbital properties are tracked. A set of four differential equations is numerically integrated, describing the evolution of orbital separation, eccentricity, and component spins, which depend on tidal interactions as well as angular momentum losses associated with magnetic braking, gravitational radiation, and stellar wind mass losses. (3) All types of mass-transfer phases are calculated: stable driven by nuclear evolution or angular momentum loss and thermally or dynamically unstable. Any system entering the Roche lobe overflow (RLOF) is assumed to become immediately circularized and synchronized. If dynamical instability is encountered the binary may enter a CE phase. For the modeling of this phase we use the standard energy balance prescription. (4) The SN explosion is treated taking into account mass loss as well as SN asymmetries (through natal kicks to NSs and BHs at birth). The distribution of the SN kick magnitudes is inferred from observed velocities of radio pulsars. For this project we use the distribution derived by Hobbs et al. (2005), which is a single Maxwellian with $\sigma = 265$ km s^{-1}. It is, however, assumed that NS formation via electron capture or accretion induced collapse does not lead to SN kicks. (5) Finally, the X-ray luminosity of accreting binaries with NS and BH primaries (both for wind-fed and RLOF systems) is calculated. For RLOF-fed systems there is a distinction made between persistent and transient (systems that undergo thermal disk instability), while wind-fed systems are always considered as persistent X-ray sources. The mass transfer is conservative up to the Eddington limit for persistent X-ray binaries, while transients are allowed to have slightly super-Eddington luminosity (up to $3 \times L_{\rm Edd}$) (Taam et al. 1997). In all cases we apply appropriate bolometric corrections ($\eta_{\rm bol}$) to convert the bolometric luminosity to the observed *Chandra* band. A much more detailed description of all code elements, treatments of physical processes and implementation is provided in Belczynski et al. (2008).

2.2. *Model Parameters for NGC 3379 and NGC 4278*

In this study we focus on trying to understand the XLF characteristics of the two elliptical galaxies NGC 3379 and NGC 4278, observed with *Chandra* and reported by Kim et al. (2006a). In the development of our models we incorporate our current knowledge about the characteristics of the stellar population in these galaxies (see Table 1). The observationally determined parameters of the stellar populations, such as their age and metallicity, or their total stellar mass, are similar for NGC 3379 and NGC 4278. This allows us to develop the same models in our simulations for both of them. Terlevich & Forbes (2002) estimated the ages and metallicities of 150 elliptical and late-type spiral galaxies using published high-quality spectral line indices. For NGC 3379 they are reporting an age of 9.3 Gyr and a metallicity of $[{\rm Fe/H}] = 0.16$, while for NGC 4278 the corresponding values are 10.7 Gyr and $[{\rm Fe/H}] = 0.14$. The two galaxies have very similar optical luminosity and assuming the same light to mass ratio, they should also have similar masses. Cappellari et al. (2006) used I-band observations from the *Hubble Space Telescope* to calculate the total stellar mass of the two galaxies and they found them to be 8.6×10^{10} and 9.4×10^{10} $M_{\odot}$ for N3379 and N4278, respectively. The ratio of the integrated LMXB X-ray luminosity to the optical luminosity is 4 times smaller for NGC 3379, which also has 6 times lower GC specific frequency compared to NGC 4278 (see Kim et al. 2006a; Ashman & Zepf 1998).

There are, however, a number of parameters in our models for which we do not have any direct guidance from observations. We have no information about the star formation history of the two galaxies, and thus we assume a δ-function–like star formation episode at time $t = 0$. Also unknown are the initial mass function (IMF) and the distributions of orbital separation and eccentricity for the primordial binary systems. We adopt two different IMFs: Scalo/Kroupa and Salpeter, while for the distributions of the orbital properties we follow the standard assumptions described in Belczynski et al. (2002). Other parameters that can affect the final LMXB population are the binary fraction of the host galaxy, the magnetic braking law adopted, and the CE efficiency ($\alpha_{\rm CE}$) The specific parameters we used to model the ellipticals NGC 3379 and NGC 4278 are listed in Table 2.

TABLE 2
MODEL PARAMETERS FOR NGC 3379 AND NGC 4278

Parameter	Notation	Value
Star formation		δ-function at $t = 0$
Population age (Gyr)		9–10
Metallicity	Z	0.03
Total stellar mass ($M_\odot$)	M_*	9×10^{10}
Binary fraction (%)	$F_{\rm bin}$	50
IMF		Scalo/Kroupa or Salpeter
CE efficiency (%)	$\alpha_{\rm CE}$	20–100
Magnetic braking		Rappaport et al. (1983) or Ivanova & Taam (2003)

We note that in our calculations we combine $\alpha_{\rm CE}$ and λ into one CE parameter, where λ is a measure of the central concentration of the donor and the envelope binding energy (see, e.g., the appendix in Justham et al. 2006). In the rest of the text, whenever we mention the CE efficiency $\alpha_{\rm CE}$, we refer in practice to the product $\alpha_{\rm CE} \times \lambda$, effectively treating λ as a free parameter (see Belczynski et al. 2008 for details). Justham et al. (2006) argued that λ-values for high-mass stars are very small (<0.1) and concluded that unreasonably high values of $\alpha_{\rm CE}$ are needed for CE ejection. However, one must take into account that λ is highly uncertain primarily because of important uncertainties in defining the core-envelope boundary in the donor. As clearly shown by Dewi & Tauris (2000) and especially by Tauris & Dewi (2001) λ-values for a 20 $M_\odot$ (10 $M_\odot$) are uncertain by factors of $\sim$70 ($\sim$20). Therefore, choosing a fixed value of λ for donors of a certain mass and evolutionary stage is a gross oversimplification. For these reasons we combine $\alpha_{\rm CE}$ and λ into one model parameter and explore reasonable values of it.

2.3. *Models for the X-Ray Luminosity Function*

In our models we keep track of all the binary properties, including the mass-transfer rate ($\dot{M}$), as a function of time for populations of accreting NS and BH. We use the mass-transfer rates to identify the persistent and transient sources in our simulation results. Binaries for mass transfer rate higher than the critical rate $\dot{M}_{\rm crit}$ for the thermal disk instability (van Paradijs 1996; King et al. 1996; Dubus et al. 1999; Menou et al. 2002) are considered persistent sources, and their X-ray luminosity ($L_{\rm x}$) is calculated directly from the mass transfer rate as

$$L_{\rm x} = \eta_{\rm bol}\epsilon\frac{GM_a\dot{M}}{R_a},$$

where the radius of the accretor (R_a) is 10 km for a NS and 3 Schwarzschild radii for a BH, ϵ gives a conversion efficiency of gravitational binding energy to radiation associated with accretion onto a NS (surface accretion $\epsilon = 1.0$) and onto a BH (disk accretion $\epsilon = 0.5$), and $\eta_{\rm bol}$ is a factor that converts the bolometric luminosity to the X-ray luminosity in the *Chandra* energy band (0.3–8 keV). For RLOF-accreting BHs this conversion factor is estimated to be $\eta_{\rm bol} = 0.8$ (Miller et al. 2001), while for RLOF-accreting NSs $\eta_{\rm bol} = 0.55$ (Di Salvo et al. 2002; Maccarone & Coppi 2003; Portegies Zwart et al. 2004). The two correction factors ϵ and $\eta_{\rm bol}$ are applied in both persistent sources and transient sources in outburst.

In the context of the thermal disk instability model, mass transferring binaries with $\dot{M} < \dot{M}_{\rm crit}$ are considered transient sources, meaning that they spend most of their life in a quiescent state ($T_{\rm quiscent}$), in which they are too faint to be detectable, and they occasionally go into an outburst. The fraction of the time that these systems are in outburst ($T_{\rm outburst}$) defines their DC:

$$\mathrm{DC} \equiv \frac{T_{\rm outburst}}{T_{\rm outburst} + T_{\rm quiescent}}. \quad (1)$$

Observations of Galactic LMXBs show that transient systems spend most of their life in the quiescent state, hinting at a DC below 20% (Tanaka & Shibazaki 1996).

The outburst luminosity and the DC of transient systems is not well understood and cannot be calculated from first principles. Instead, we have to rely primarily on empirical constraints and simple theoretical arguments. In our analysis we consider a number of different treatments of these parameters for transients, which we describe in what follows.

As a first approximation it has been suggested that transient LMXBs emit at their Eddington luminosity ($L_{\rm Edd}$) when they are in outburst. In a different approach Portegies Zwart et al. (2005) derived an empirical correlation between the outburst luminosity of Milky Way transient LMXBs with BH accretors and their orbital period P:

$$L_{\rm x} = \eta_{\rm bol}\epsilon \times \min\left[2 \times L_{\rm Edd},\ 2 \times L_{\rm Edd}\left(\frac{P}{10\ \mathrm{hr}}\right)\right]. \quad (2)$$

We can generalize this relation to all transient LMXBs in galaxies other than our own, but we note that there has not been any observational work that shows that NS-LMXBs follow a similar trend.

A more physical treatment is to assume that in the quiescent state the compact object does not accrete (or accretes an insignificant amount of mass) and matter from the donor is accumulated in the disk. In the outburst state all this matter is accreted onto the compact object emptying again the disk. Taking into account as well that the X-ray luminosity probably cannot exceed $L_{\rm Edd}$ by more than a factor of 2 (see Taam et al. 1997), we end up with a definition of the outburst luminosity as

$$L_{\rm x} = \eta_{\rm bol}\epsilon \times \min\left(2 \times L_{\rm Edd},\ \frac{GM_a\dot{M}_d}{R_a}\frac{1}{\mathrm{DC}}\right) \quad (3)$$

In the equation above, DC is unknown. Dobrotka et al. (2006) studied accretion disk models for cataclysmic variables that are thought to experience the same thermal disk instability (dwarf novae). They found a correlation between the DC of the system and the rate at which the donor star is losing mass $\dot{M}_d$. The exact relation of these to quantities depends on the values of the disk's viscosity parameters, but the general behavior can be approximated by

$$\mathrm{DC} = \left(\frac{\dot{M}_d}{\dot{M}_{\rm crit}}\right)^2. \quad (4)$$

Plugging equation (4) into equation (3) we eliminate the DC dependence and get an expression for the outburst luminosity of a transient system that depends only quantities which are directly calculated in our population modeling:

$$L_{\rm x} = \eta_{\rm bol}\epsilon \times \min\left(2 \times L_{\rm Edd},\ \frac{GM_a\dot{M}_{\rm crit}^2}{R_a\dot{M}_d}\right). \quad (5)$$

The accretion disk models by Dobrotka et al. (2006) assume accretion onto a compact object with a hard surface and it is not obvious that the same results will apply for accretion onto a BH.

In order to take into account all the available information, empirical and theoretical, about LMXB transient behavior, we treat BHs and NS-LMXBs differently and define the outburst luminosity as

$$L_{\rm x} = \eta_{\rm bol}\epsilon \begin{cases} \min\left[2\times L_{\rm Edd}, 2\times L_{\rm Edd}\left(\dfrac{P}{10\ {\rm hr}}\right)\right], & \text{for BH acc,} \\ \min\left(2\times L_{\rm Edd}, \dfrac{GM_a\dot{M}_{\rm crit}^2}{R_a\dot{M}_d}\right), & \text{for NS acc.} \end{cases} \quad (6)$$

We note that for BH-LMXBs, we adopt a single DC value for simplicity and lack of other information, although we have no clear physical reason to believe that all BH systems have the same DC. It is believed that the DC of BH systems is smaller than that of NS systems, on the order of 5% (Tanaka & Shibazaki 1996). We found that in all our models NS accretors greatly outnumber BH accretors. BH systems only have an important contribution at high luminosities, where the error bars in the observed XLFs (see Kim et al. 2006a) are too large to give us any tight constraints for our models. As we show in § 3.1, the treatment described in equation (6) gives us the best agreement with observations.

To construct the XLF we consider a snapshot of the whole population at the time we are interested in and we identify the LMXBs as transient or persistent. If a system is transient we decide whether it is in outburst or in quiescence according to its DC and either assign an outburst luminosity or discard the system as quiescent and hence too faint to contribute to the XLF. We then construct the XLF by calculating the cumulative X-ray luminosity distribution of the sources that are detectable (persistent and transient in outburst). We note that the age of the elliptical galaxies NGC 3379 and NGC 4278, and hence their LMXB population, is known only to within ∼1 Gyr. Consequently, we cannot just choose a unique snapshot of the population. Instead, we construct the XLF by considering the time window of 9–10 Gyr, divided into time slices of 1 Myr. We construct the XLF at each of these time slices, and we take the average to represent the XLF that corresponds to the time window of interest. By doing this, we also improve the statistics of our model sample.

It is computationally impossible to evolve enough binaries to correspond to the total initial number of binaries in an elliptical galaxy ($\sim 10^9$ binaries). For each model we evolve 10^6 binaries, which takes about 2 months of CPU time on a modern processor. We then normalize to the total mass of the galaxy in question, taking into account the initial binary fraction and the IMF.

3. RESULTS

3.1. *Exploring the Parameter Space*

One of the implicit weaknesses of PS models is the large number of free parameters that one can vary and fine-tune in order to get the desirable result. There are physical processes involved in the evolution of a binary system, such as stellar winds and magnetic braking, which are not fully understood. In this case various prescriptions are typically used to model them. Fortunately, (1) the result of interest to us in this study (XLF) is not sensitive to all of these model parameters, and (2) we can use some empirical knowledge from observations to constrain these parameters. We study a total of 336 models. In Table 3 we list 28 combinations of PS input parameters we study (CE efficiency, IMF, wind strength), and in Table 4 we list the six different prescriptions we use for the determination of the DC and outburst luminosity of transient LMXBs. For each of the parameter combination from Tables 3 and 4, we try two prescriptions for the magnetic braking law, by Ivanova & Taam (2003) and Rappaport et al. (1983). Parameters not mentioned here are set as in the standard model considered in Belczynski et al. (2008). We name our models using a combination of a number from Table 3, which denotes the PS parameters of the models, a letter from Table 4, which denotes the prescription we use for the treatment of transient LMXBs, and a superscript that denotes the magnetic braking law used.

TABLE 3
Population Synthesis Models

Model	$\alpha_{\rm CE}$	IMF	$\eta_{\rm wind}$
1	0.2	Salpeter	0.25
2	0.2	Scalo/Kroupa	0.25
3	0.2	Salpeter	1.0
4	0.2	Scalo/Kroupa	1.0
5	0.3	Salpeter	0.25
6	0.3	Scalo/Kroupa	0.25
7	0.3	Salpeter	1.0
8	0.3	Scalo/Kroupa	1.0
9	0.4	Salpeter	0.25
10	0.4	Scalo/Kroupa	0.25
11	0.4	Salpeter	1.0
12	0.4	Scalo/Kroupa	1.0
13	0.5	Salpeter	0.25
14	0.5	Scalo/Kroupa	0.25
15	0.5	Salpeter	1.0
16	0.5	Scalo/Kroupa	1.0
17	0.6	Salpeter	0.25
18	0.6	Scalo/Kroupa	0.25
19	0.6	Salpeter	1.0
20	0.6	Scalo/Kroupa	1.0
21	0.7	Salpeter	0.25
22	0.7	Scalo/Kroupa	0.25
23	0.7	Salpeter	1.0
24	0.7	Scalo/Kroupa	1.0
25	1.0	Salpeter	0.25
26	1.0	Scalo/Kroupa	0.25
27	1.0	Salpeter	1.0
28	1.0	Scalo/Kroupa	1.0

Notes.—For each of the models listed below we applied two magnetic braking law prescriptions. In the rest of the text the Ivanova & Taam (2003) prescription is denoted with the IT superscript at the end of the model name, and the Rappaport et al. (1983) prescription with the RVJ superscript.

The analysis of several population simulations enables us to identify general behaviors of how the LMXB population is affected by changes to different parameters. In Figure 1 we show the modeled XLFs for 36 selected models, separated in six panels. In each panel all the parameters that determine the formation and evolution of LMXBs are kept constant, and we just change the modeling of transient systems (their DC and outburst luminosity). The observed XLFs of the two galaxies, NGC 3379 and NGC 4278, are also plotted for comparison.

We find that the stellar wind strength significantly alters only the BH-LMXB population and thus only the high-luminosity region of the modeled XLF. Stellar winds are important mainly in the evolution of massive stars, which, depending on the wind prescription assumed, may lose a significant part of their envelope. Weaker stellar winds result in more massive presupernova cores and thus to the formation of more BHs. On the other hand, the IMF affects the LMXB population globally. A flatter (Salpeter) IMF increases the overall number of sources with luminosities above 10^{37} ergs s^{-1}, but still gives results consistent with the observations. The modeled XLF is more sensitive to the CE

TABLE 4
TREATMENT OF TRANSIENT LMXBS

Model Name	$L_{x,NS}$	$L_{x,BH}$	DC_{NS}	DC_{BH} (%)
A	Eq. (6)	Eq. (6)	Eq. (4)	5
B	Eq. (3)	Eq. (3)	1%	1
C	Eq. (3)	Eq. (3)	7%	7
D	Eq. (3)	Eq. (3)	15%	15
E	L_{Edd}	L_{Edd}	10%	10
F	Eq. (2)	Eq. (2)	10%	10

NOTE.—We tried six different prescriptions for the determination of the DC and outburst luminosity of transient LMXBs.

efficiency α_{CE}. Smaller α_{CE} values lead to more mergers among LMXB progenitors and therefore decrease the overall formation rate of LMXBs. If the CE efficiency is set to a very small value ($\alpha_{CE} < 0.2$), it becomes very difficult to form any LMXBs at all (Kalogera & Webbink 1998), while a high CE efficiency $\alpha_{CE} > 0.6$ clearly overproduces LMXBs. It is also clear that the adopted magnetic braking law greatly affects the characteristics of the model LMXB population. The XLFs of all 336 models can be seen in the online material supplemental to this paper.

The ratio of persistent to transient LMXBs produced from our models, including systems both in outburst and in quiescence, is on the order of 1:20. So even if transient systems have a small DC (DC < 10%), their contribution to the shape of the XLF is important and some times they may even dominate the population (as discussed by Piro & Bildsten [2002]). From this simple argument, we can understand that the shape of the modeled XLFs should be very sensitive to the DC and the outburst luminosity of transient systems. Figure 1 confirms this last statement, as we see that the larger variation in the shape of the modeled XLFs comes from different prescriptions in the treatment of transient systems and not from changing the binary evolution parameters.

We compare quantitatively our modeled XLFs to the observed ones from the two elliptical galaxies NGC 3379 and NGC 4278, using statistical tests that make no a priori assumption about the functional form of the observed XLF, and we report the

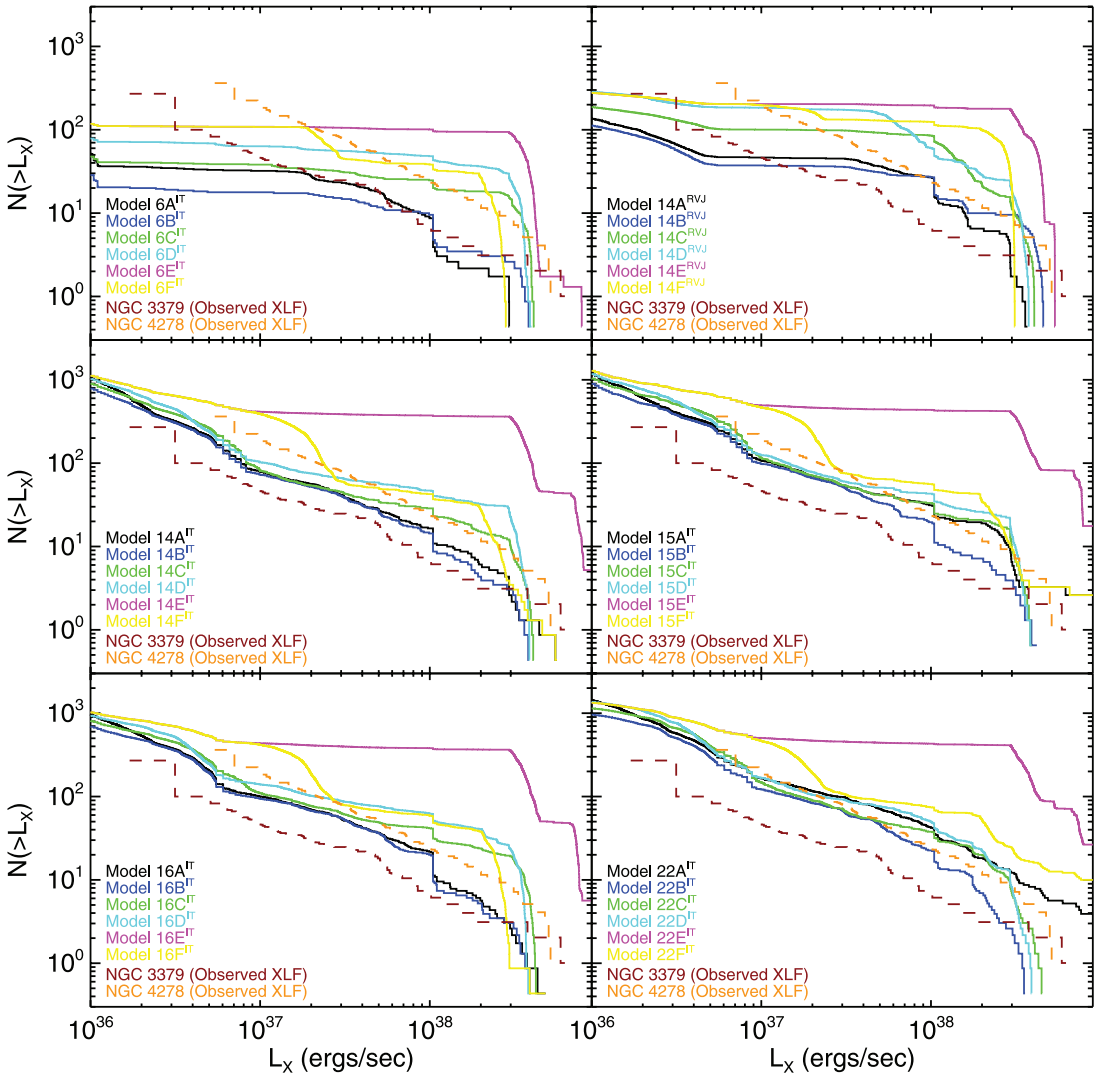

FIG. 1.—Model XLFs for 36 selected LMXB population. In each panel all the PS parameters are kept constant, and only the modeling of transient systems changes. For comparison the observed XLFs of NGC 3379 (*dark red*) and of NGC 4278 (*orange*) are drawn. In our statistical comparison we included only systems with luminosity above the completeness limit for the specific observations ($>10^{37}$ ergs s^{-1} for NGC 3379 and $>3 \times 10^{37}$ ergs s^{-1} for NGC 4278). The modeling of the transient systems and their outburst characteristics can be more important than the usual PS parameters; commonly used assumptions such as assigning the outburst luminosity of the transient LMXBs to be equal to L_{Edd} (transient treatment E) lead to XLFs clearly inconsistent with the observations. [*See the electronic edition of the Journal for additional panels of this figure*.]

TABLE 5
STATISTICAL COMPARISON OF MODELS TO THE OBSERVED XLF OF NGC4278

MODEL	NGC 3379				NGC 4278			
	P_{KS}	P_{Kuiper}	P_{χ^2}	P_{RS}	P_{KS}	P_{Kuiper}	P_{χ^2}	P_{RS}
$6A^{IT}$	0.037	0.065	0.006	0.022	**0.275**	0.020	**0.202**	0.046
$6B^{IT}$	2.18E−04	0.002	5.63E−05	1.53E−04	0.002	0.007	0.012	3.92E−04
$6C^{IT}$	3.89E−08	1.10E−07	7.75E−07	1.10E−06	4.89E−09	7.27E−09	5.96E−08	1.04E−09
$6D^{IT}$	1.61E−13	1.68E−13	0.00E+00	5.48E−11	4.67E−15	1.12E−15	0.00E+00	1.33E−15
$6E^{IT}$	1.40E−24	7.98E−25	0.00E+00	0.00E+00	5.03E−34	1.31E−35	0.00E+00	0.00E+00
$6F^{IT}$	0.001	1.60E−05	0.011	0.00E+00	6.60E−13	1.97E−16	0.00E+00	7.46E−11
$14A^{RVJ}$	2.77E−07	6.89E−07	0.00E+00	4.96E−10	3.34E−04	1.30E−04	0.003	6.39E−04
$14B^{RVJ}$	1.34E−10	3.33E−10	0.00E+00	2.93E−10	2.60E−08	3.35E−08	5.13E−06	4.68E−07
$14C^{RVJ}$	4.94E−19	1.83E−19	0.00E+00	0.00E+00	3.61E−18	2.11E−19	0.00E+00	0.00E+00
$14D^{RVJ}$	6.87E−10	5.52E−10	0.00E+00	0.00E+00	6.96E−06	1.25E−06	4.06E−04	1.03E−10
$14E^{RVJ}$	6.72E−27	6.11E−28	0.00E+00	0.00E+00	5.05E−37	2.14E−35	0.00E+00	0.00E+00
$14F^{RVJ}$	4.38E−10	3.35E−10	2.38E−07	0.00E+00	3.17E−24	3.97E−29	0.00E+00	0.00E+00
$14A^{IT}$	**0.804**	**0.553**	**0.351**	**0.528**	**0.661**	**0.654**	**0.302**	**0.438**
$14B^{IT}$	**0.780**	**0.785**	**0.291**	**0.536**	**0.890**	**0.779**	**0.462**	**0.449**
$14C^{IT}$	0.049	0.045	**0.171**	0.018	3.24E−05	4.32E−05	3.29E−04	3.36E−04
$14D^{IT}$	1.70E−04	3.22E−04	0.001	0.002	1.14E−08	5.67E−09	0.00E+00	2.76E−08
$14E^{IT}$	3.82E−28	3.38E−25	0.00E+00	0.00E+00	0.00E+00	0.00E+00	0.00E+00	0.00E+00
$14F^{IT}$	1.95E−06	5.16E−06	0.001	0.00E+00	2.21E−08	3.94E−09	1.31E−06	4.57E−07
$15A^{IT}$	**0.193**	**0.303**	**0.199**	0.065	0.001	0.004	0.002	2.36E−04
$15B^{IT}$	**0.871**	**0.647**	**0.366**	**0.444**	**0.837**	**0.509**	**0.483**	0.066
$15C^{IT}$	**0.298**	**0.151**	**0.454**	0.035	2.92E−04	5.57E−04	9.97E−04	5.96E−05
$15D^{IT}$	0.052	0.042	**0.194**	0.010	2.04E−07	2.11E−07	2.86E−06	2.87E−07
$15E^{IT}$	1.72E−26	1.51E−23	0.00E+00	0.00E+00	1.96E−44	2.61E−41	0.00E+00	0.00E+00
$15F^{IT}$	4.27E−06	1.28E−06	0.005	1.11E−16	4.95E−09	2.47E−08	1.19E−07	1.67E−07
$16A^{IT}$	**0.832**	**0.778**	**0.294**	**0.397**	**0.498**	**0.121**	**0.377**	0.022
$16B^{IT}$	**0.585**	**0.629**	**0.204**	**0.471**	**0.276**	**0.129**	**0.328**	0.007
$16C^{IT}$	0.009	0.018	0.044	0.004	5.22E−07	3.61E−07	3.91E−05	6.95E−07
$16D^{IT}$	1.91E−04	3.26E−04	0.001	0.003	1.54E−09	1.16E−10	0.00E+00	8.82E−08
$16E^{IT}$	8.10E−26	5.55E−23	0.00E+00	0.00E+00	6.45E−44	3.10E−41	0.00E+00	0.00E+00
$16F^{IT}$	2.78E−05	9.86E−06	0.008	4.44E−16	1.43E−10	1.57E−13	1.79E−07	3.03E−09
$22A^{IT}$	**0.184**	**0.566**	0.095	**0.606**	0.045	**0.103**	0.035	**0.358**
$22B^{IT}$	**0.887**	**0.921**	**0.331**	**0.793**	**0.845**	**0.575**	**0.442**	**0.426**
$22C^{IT}$	**0.424**	**0.122**	**0.408**	0.046	0.003	7.28E−04	0.025	0.019
$22D^{IT}$	0.041	0.020	**0.160**	0.090	3.17E−05	9.40E−06	2.01E−04	6.87E−04
$22E^{IT}$	6.17E−25	2.35E−22	0.00E+00	0.00E+00	3.48E−43	2.40E−40	0.00E+00	0.00E+00
$22F^{IT}$	2.66E−04	6.07E−05	0.005	2.66E−11	1.46E−09	1.13E−08	0.00E+00	4.51E−06

NOTES.—Table 5 is published in its entirety in the electronic edition of the *Astrophysical Journal*. A portion is shown here for guidance regarding its form and content. We used four different statistical tests for each case (Kolmogorov-Smirnov test, Kuiper test, Wilcoxon rank-sum test and χ^2 goodness of fit test) and we are listing the probabilities, derived from each test, that a modeled XLF is consistent with the observed ones. For the statistical comparison of the complete list of models please see the electronic supplemental material.

probability that the two data sets are drawn from the same distribution. In order to make a fair comparison between models and observations, we include in our statistical analysis only systems with luminosity above the completeness limit for the specific observations ($>10^{37}$ ergs s^{-1} for NGC 3379 and $>3 \times 10^{37}$ ergs s^{-1} for NGC 4278). We have used three hypothesis-testing statistical methods, the widely used Kolmogorov-Smirnov (KS) test, the Kuiper test, which is a variation of the KS that is equally sensitive in the whole range of the XLF and not only in the mid-range, and the Wilcoxon rank-sum (RS) test. We have also used the χ^2 goodness-of-fit test (Press et al. 2007). We note here that all four statistical tests compare only the shape of the XLFs and not their absolute normalization.

In Table 5 we list the *P*-values (the probability that the two data sets are drawn from the same distribution) for all four tests, comparing the models shown in Figure 1 with each of the two observed XLFs from NGC 3379 and NGC 4278. For the statistical analysis of the complete list of models examined in this work, please see the online supplemental material. We use this analysis to draw general conclusions regarding the behavior of our models. In all cases, when we assume the outburst luminosity of the transient LMXBs to be equal to L_{Edd} or use equation (2) (transient treatment E and F; see Table 4), the *P*-values are extremely low, and we can confidently say that this treatment of transient systems is highly unlikely to be correct. Assigning the same constant DC to all transients and then calculating the outburst luminosity using equation (3) sometimes leads to results consistent with the observations, depending on the rest of the parameters used in the models. When this constant DC is as low as 1% (transient treatment B), the modeled XLFs resemble remarkably the observed ones. This happens because such a low DC practically removes the contribution of transient LMXBs to the total XLF. However, a DC of 1% is unrealistically low, based on both observational evidence and theoretical predictions. Finally, the transient treatment A consistently provides the best agreement with observations, and in addition it is the one most physically motivated. One of our primary conclusions from this analysis is that careful modeling of the transient systems and their outburst characteristics is very important, more important than the usual PS parameters.

In studying the complete list of models (see online supplemental material) it becomes evident that the magnetic braking law applied during the evolution of the LMXBs drastically changes the resulting population. Models in which the Rappaport et al. (1983) prescription is used produce XLFs inconsistent with the observations. The Rappaport et al. (1983) braking-law prescription predicts much stronger angular momentum losses compared to the Ivanova & Taam (2003) one. Very strong angular momentum loss due to magnetic breaking lead to population of LMXBs in which only wide binaries have avoided a possible merger. Our findings in favor of a milder magnetic braking law (Ivanova & Taam 2003) are in agreement with earlier work by Kalogera et al. 1998 and references therein). On the other hand, we found that the stronger Rappaport et al. (1983) prescription produces a flatter XLF at low luminosities and a break at $\sim 5 \times 10^{37}$ ergs s^{-1}. This break has been observed in some early-type galaxies (Fabbiano 2006 and references therein). The model XLFs presented in this paper that show this feature are clearly inconsistent with observations. However, they suggest that the XLF breaks at $\sim 5 \times 10^{37}$ ergs s^{-1} seen in some galaxies are produced by the magnetic braking mechanism.

Our statistical analysis tests only the shape of the XLF. However, within the uncertainties of the total mass of the two galaxies most of models we consider turn out to have the right normalization, and therefore this is not a strongly discriminating constraint. We note also that the PS model normalization can be very sensitive to certain binary evolution parameters, such as the distribution of the mass ratios between the initial masses of the two binary components. Without a proper multidimensional coverage of the parameter space, and given the uncertainties in the total galaxy mass, we cannot use the total number of LMXBs observed as a formal constraint. Instead, we remain satisfied that most of the models we consider give us a total number of LMXBs in the observed luminosity regime, with a factor of 3 from the observed sample. This factor is comparable to the galaxy mass uncertainty (Cappellari et al. 2006).

In the discussion that follows we use model 14A$^{\rm IT}$ as our *standard* model, which gives an XLF closest both in shape and normalization to the observed ones.

3.2. *Analyzing the LMXB Population*

In order to investigate further the characteristics of our modeled LMXB population, we classify the LMXBs based on their donor stellar type and also separate them into transient and persistent systems (Fig. 2). We also examine the orbital periods of each subpopulation. This way we can infer to what degree each subpopulation contributes to the total XLF. For our *standard* model 14A$^{\rm IT}$ we find that systems with MS donors are the most numerous group, but their luminosity usually falls below the detection limit ($\sim 3 \times 10^{36}$ ergs s^{-1}). The XLF is dominated by transient and persistent systems with red giant donors, which, despite being less numerous overall, are more luminous. It is worth pointing out that the population of ultracompact LMXBs with WD donors, which Bildsten & Deloye (2004) argued dominate the LMXBs in GCs, is also present in our models. Their semianalytically derived XLF has, as expected, the same shape as the one found in our models (power law with a slope of -0.8). We find in our models that the number of these systems formed in the galactic fields can be comparable to the number of LMXBs with red giant donors, but most of the time their contribution to the XLF is masked by the red giant donor systems.

We note here that the observed XLFs tend to get flatter at low luminosities ($<10^{37}$ ergs s^{-1}). At this luminosity range our model XLFs are dominated by LMXBs with MS donors, and some of the models actually show the opposite trend (i.e., steepening of the XLF at low luminosities). However, we are not able to use this feature of the observed XLFs as a constraint to our models, as it falls below the completeness limit of the observations and a direct statistical comparison is not valid in this regime.

LMXBs with NS accretors outnumber those with a BH accretor by a factor of $\sim$50. A small population of transient BH-LMXBs makes a significant contribution only to the high-luminosity end of the XLF, above 2×10^{38} ergs s^{-1}. These transient BH-LMXBs have orbital periods from 1 to 10 hr and luminosity comparable to the Eddington luminosity given in equation (6), which we adopted in this model. We also find a subpopulation of persistent BH-LMXBs with MS donors, but their luminosity falls below the observational limit of the *Chandra* observations.

We performed the same analysis for all of our models (plots similar to Fig. 2 for all models can be found in the online supplemental material), and we identified some general trends on how the different PS parameters affect the LMXB population. The strongest effect comes from variation of the CE efficiency $\alpha_{\rm CE}$. Low CE efficiencies ($\alpha_{\rm CE} < 0.3$) result to the merger of all low-period systems, and only the widest binaries avoid a merger and survive the CE phase. Such wide binaries become wide-orbit LMXBs with red giant donors. In models with higher CE efficiencies, binaries with progressively tighter orbits survive the CE phase, and we see LMXBs with shorter period and WD or MS donors appearing in our current population. Although these systems become more numerous for $\alpha_{\rm CE} > 0.4$, LMXBs with red giant donors still make the most important contribution to the XLF for luminosities above 10^{37} ergs s^{-1}. We note that models of Galactic X-ray binary populations usually favor $\alpha_{\rm CE}$ in the range 0.3–2.0 (Taam & Sandquist 2000; Kalogera & Webbink 1998; Kalogera et al. 1998, and references therein).

The IMF affects the global picture of the LMXB population too. A flatter IMF (Salpeter) favors the formation of more massive stars. On the one hand, this leads to the formation of BH-LMXBs and, on the other, favors the formation of generally more massive secondary stars which have evolved into WD by the time the system reaches the LMXB phase. We find that models with steep IMF (Scalo/Kroupa) have less LMXBs with WD donors than models with the same initial parameters but a flatter IMF (Salpeter). The stellar wind strength has similar effects on the LMXB population, as it affects the mass of the two components and thus their evolutionary state when they reach the LMXB phase. This effect is more prominent in the massive primary stars, where strong wind mass loss leads to less massive presupernova cores and thus fewer BHs.

Two of the PS parameters we varied in study (IMF and stellar wind strength) greatly affect the formation of BH-LMXBs. Therefore, some of our models (those with steep IMFs and strong stellar winds) turn out to be highly inefficient in the formation of BH-LMXBs. However, a population of LMXBS with only NS accretors cannot form sources with luminosities reaching up to 10^{39} ergs s^{-1} unless we assume that highly super-Eddington accretion onto NSs is possible. Consequently, forming enough BH-LMXBs to populate the very high end of the XLF is a discriminative criterion for our models.

3.3. *Time Evolution of the LMXB Population*

The age of the population is a very important factor in our simulations, as the characteristics of the binaries and their relative

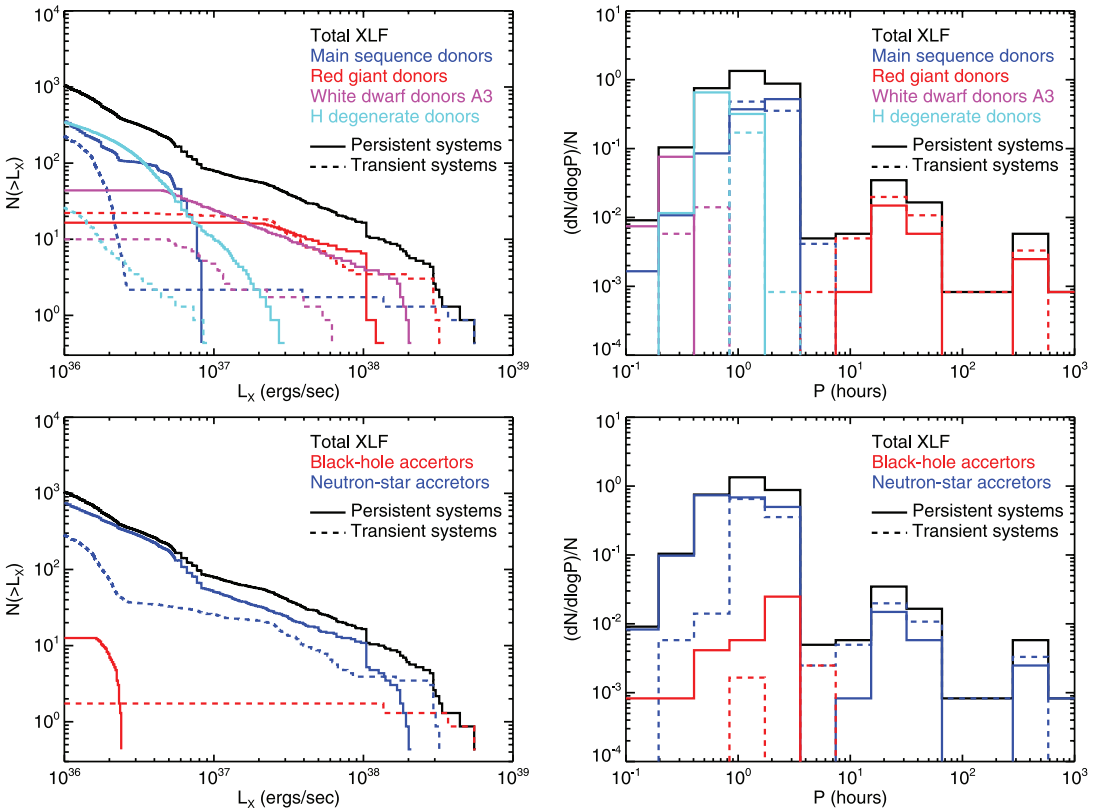

FIG. 2.—Analysis of the LMXB population. We show the contribution of different subpopulations by separating the LMXBs into groups of systems with different donor (*top left*) and accretor (*bottom left*) stellar types. We find that the midrange of the XLF is dominated by NS-LMXB with red giant donors, while the high end is dominated by BH LXBs with MS donors. Using the same separation into subpopulations we show the probability density function of the orbital period P of groups with different donor (*top right*) and accretor (*bottom right*) stellar types. [*See the electronic edition of the Journal for additional panels of this figure.*]

numbers and contributions vary significantly over time. In the right panel of Figure 3 we see the evolution of the modeled XLF versus time. The total number of sources, as well as the number of luminous sources, decreases steadily with time. At early times, the first 5 to 6 Gyr, the XLF receives significant contributions from intermediate-mass X-ray binaries. The increased number of luminous sources at earlier times makes the shape of the XLF flatter. At the other extreme, in a 13 to 14 Gyr old stellar population, the population of luminous LMXBs is almost nonexistent. These results are in agreement with the qualitative predictions made by Wu (2001) using a simple birth-death model. The formation rate of X-ray binaries in general, and of persistent sources in particular, can be seen in right panel of Figure 3. The two curves follow each other closely, which means that according to our models, most the X-ray binaries go through a phase of persistent emission at some point of their evolution. Another characteristic that initially might seem counterintuitive is that after a peak in the production of X-ray binaries in the first few gigayears, there is a decreasing but *steady* production of *new* persistent systems, even after 10 or 11 Gyr. This suggest that there can be a very long delay between the formation of the compact object (at ~1–100 Myr) and the onset of the mass-transfer phase. We should note that the derivation of the ages of the two galaxies by Terlevich & Forbes (2002) involves a

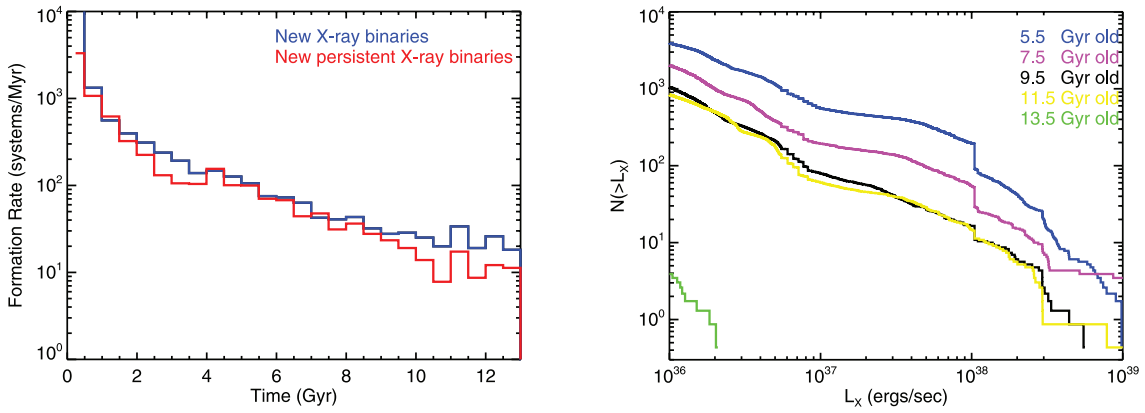

FIG. 3.—*Left*: Formations rate of all X-ray binaries (*blue line*) and only of persistent X-ray binaries (*red line*) as a function of time. After a peak in the formation rate for the first few gigayears, there is a decreasing but steady production of new persistent systems even after 10 or 11 Gyr. *Right*: Evolution of the XLF with the age of the galaxy.

systematic uncertainty of at least 1 Gyr. This uncertainty in the age is an additional factor that can account for the difference in the number of observed sources between the two galaxies and of course for some deviation between the observed and the modeled XLFs.

3.4. *The Implication of GCs in the LMXB Population: NGC 3379 vs. NGC 4278.*

The simulations we present in this initial study do not take into account formation channels involving dynamical interactions, which are believed to dominate the formation of LMXBs in GCs. However, we know from comparisons of optical and X-ray observations that 10%–70% of LMXBs in early-type galaxies are located in GCs, depending on the type of the galaxy and the GC-specific frequency (Kundu et al. 2007; Jordán et al. 2004; Sarazin et al. 2003). It is thus clear that at least for some galaxies, the LMXB formation in GC makes an important contribution to the total population. Fabbiano et al. (2007) studied the GC LMXB population of NGC 3379 and found that only 15% of all LMXBs detected in this galaxy coincide with GCs. Furthermore, they argued that there are differences in the XLF of the two populations of field and GC LMXBs, but *only* at low luminosities (below 10^{37} ergs s^{-1}), where the incompleteness of the observed population does not allow reliable direct comparison with theoretical models. Thus, it turns out that it is valid to compare our models to the total observed XLF (without subtracting the GC LMXBs) of NGC 337 for luminosities above 10^{37} ergs s^{-1}. The case of NGC 4278 is different, as its GC-specific frequency is 5 times larger than that of NGC 3379, and the contribution of GC LMXBs is expected to be more significant there. An analysis similar to that of Fabbiano et al. (2007) for NGC 3379 will appear in the near future, and it will enable us to separate the field from the GC LMXB population in our comparison.

The realistic modeling of X-ray binaries formed in GCs requires the coupling of cluster dynamics with binary evolution. Bildsten & Deloye (2004) suggested that ultracompact X-ray binaries dominate the cluster population and that they are continuously replenished through dynamical interactions. These systems initially evolve through a bright persistent phase (for 3 Myr), then their mass transfer rate drops gradually as the WD donor mass decreases; the systems become transients and their contribution to the XLF is diminished. Our models for formation of LMXBs from primordial binaries produce a population of ultracompact binaries too. Not surprisingly, since the properties of the binaries are very similar, the XLF of this subpopulation has the exact same shape as the one produced by the model of Bildsten & Deloye (2004): a power-law–shaped XLF (slope of -0.8) slightly flatter than the observed XLF of NGC 3379 and NGC 4278. In the case of the galactic field population, however, there is no enhancement in the formation rate of these systems via dynamical interactions. So our models do not produce enough luminous persistent systems to dominate the total XLF. Their contribution, although significant, is usually masked by LMXBs with red giant donors, which tend to have higher X-ray luminosities. More recently, Ivanova et al. (2008) studied the formation of compact binaries containing NSs in dense GCs. In their simulations they used StarTrack as their PS model and adopted a simplified treatment of the dynamical events (see also Ivanova & Kalogera 2006). They found that formation rate of dynamically formed LMXBs with red giant and MS donors is comparable to the ultracompact X-ray binaries formed in GCs, but the later ones have significantly shorter lifetimes. This last result casts doubts on the suggestion by Bildsten & Deloye (2004) for an ultracompact X-ray binary–dominated population in GCs.

4. CONCLUSIONS AND DISCUSSION

The recent deep *Chandra* observations (Kim et al. 2006a) of the two typical old elliptical galaxies: NGC 3379 and NGC 4278, led to the first observed low-luminosity XLFs of LMXBs, with the detection limit (3×10^{36} ergs s^{-1}) being about an order of magnitude lower than in most previous surveys. Motivated by this observational work, we developed PS simulations of LMXBs appropriate for these two galaxies. We considered the formation of LMXBs only through the evolution of primordial binaries in the galactic fields and examined the possible contribution to the overall LMXB population. For our modeling we used the updated PS code StarTrack (Belczynski et al. 2008).

Our main conclusions can be summarized as follows: We found that some of our models produce XLFs in very good agreement with the observations, based on both the XLF shape and absolute normalization. There is no unique combination of PS parameters and modeling of transient sources (DC and outburst luminosity) that gives an XLF in agreement with the observation. We conclude that the formation of LMXBs in the galactic field via the evolution of primordial binaries can make a significant contribution to the total population of an elliptical galaxy, especially to the ones with low GC-specific frequency such as NGC 3379 (Fabbiano et al. 2007). Nevertheless, we are able to exclude the majority of our models as inconsistent with the observations. Note that widely used, simple assumptions—such as all transient sources in the outburst state emit X-rays at $L_{\rm Edd}$—lead to XLFs that are clearly inconsistent with the observed ones. Our results appear to be robust, since we do not have to fine-tune our code parameters in order to get a model that resembles the observed population.

As already suggested by Piro & Bildsten (2002) the LMXB population receives a significant contribution from transient systems (characterized by thermal disk instability), and with reasonable outburst DCs they can even dominate the XLF. As a consequence, the XLF shape is rather sensitive to the treatment of these transient systems. In Figure 1 we show that keeping the same PS parameters and changing *only* the modeling of transient sources leads to completely different XLFs. We tried different methods of modeling the outburst characteristics of transient LMXBs, with the following findings: (1) When we assume the outburst luminosity of all transient LMXBs to be equal to $L_{\rm Edd}$ (transient treatment E) or apply equation (2) (transient treatment F)—which was empirically derived for Galactic BH-LMXBs—to the whole population, we get XLFs inconsistent with the observed ones regarding both their shape and the total number of sources predicted. (2) A constant DC for all systems, although not physically motivated, can sometimes be a good first approximation. (3) We get the best agreement with observations when we consider a variable DC for NS-LMXBs, based on the theoretical study of Dobrotka et al. (2006; see eqs. [4] and [5]), while for the BH-LMXBs we use the empirical correlation between orbital period and outburst luminosity derived by Portegies Zwart et al. (2005; see eq. [2]), assuming a low constant DC ($\sim$5%).

The LMXB subpopulations that mainly contribute to the model XLFs are NS-LMXBs with red giant donors and BH-LMXBs with MS donors. A population of persistent ultracompact LMXBs with WD donors is also present in our models and in some cases makes an important contribution too (see models $9A^{IT}$, $11A^{IT}$, and $12A^{IT}$). Of these subpopulations, the NS-LMXBs are the

most dominant, and they primarily determine the XLF shape in the medium- and low-luminosity range (below 2×10^{38} ergs s^{-1}), while the BH-LMXBs make a significant contribution to the high end of the XLF.

The normalization of the modeled XLFs is less robust as a characteristic than its shape. We normalize the models so that the number of the primordial binaries we evolve corresponds to the known galaxy masses, given the IMF and the binary fraction. There are, however, uncertainties of the order of a few in the determination of the mass of the observed galaxies, due to uncertainties in their distance, the bolometric luminosity, and the light-to-mass ratio. The majority of the models presented here produce the observed number of LMXBs to within a factor of 3, consistent with the galaxy mass uncertainties. Exceptions are models with transient treatment E or F (see Table 4) and models with high CE efficiencies (models 21–28; see 3), which greatly overproduce high-luminosity LMXBs. Furthermore, small changes in the CE efficiency can change the total number of sources produced by a model by a factor of 2, without significantly changing the shape of the XLF (compare, for example, models 10A^{IT}, 14A^{IT}, and 18A^{IT} in the online supplemental material). In view of these uncertainties and the limited parameter space available for exploration in our models, we consider this normalization agreement satisfactory, but do not use it as an actual constraint on the models.

We do not claim that the work presented in this paper is a complete PS study of field LMXBs in elliptical galaxies. It is meant to be a first effort at interpreting the recent deep *Chandra* observations of the two elliptical galaxies NGC 3379 and NGC 4278. Throughout the paper we identify the caveats qualifying our analysis, and we intend to address them in our future work. It turns out that the realistic treatment of the outburst properties of transient LMXBs is crucial for the modeling of XLFs of extragalactic populations. The derivation of an empirical correlation between the outburst luminosity and the period of Galactic NS-LMXBs, similar to the one derived by Portegies Zwart et al. (2005) for Galactic BH-LMXBs, will provide a better understanding of the differences in the transient behavior of these two classes of X-ray sources. Another simplifying assumption we made was to neglect the variation of the X-ray luminosity during an outburst event of a transient LMXB, considering it to be a second-order effect. The use of model light curves for the outburst phases of transient XLFs may affect the shape of the modeled XLFs. However, without proper observational constraints this would simply add an essentially free parameter to our simulations. We note that most of our models produce many systems with X-ray luminosity below the observational limit, down to 10^{35} ergs s^{-1}. The integrated diffuse X-ray emission from these galaxies can put a strong constraint on our models. The total luminosity of the observed diffuse emission will also include emission from gas and stellar coronae (Pellegrini & Fabbiano 1994; Revnivtsev et al. 2007) and thus must be higher than the integrated luminosity of all the LMXBs in our models with luminosities below the observational detection limit.

This work was supported by *Chandra* G0 grant G06-7079A (PI: G. Fabbiano) and subcontract G06-7079B (PI: V. Kalogera).

REFERENCES

Ashman, K. M., & Zepf, S. E. 1998, Observatory, 118, 387
Belczynski, K., Kalogera, V., & Bulik, T. 2002, ApJ, 572, 407
Belczynski, K., Kalogera, V., Rasio, F. A., Taam, R. E., Zezas, A., Bulik, T., Maccarone, T. J., & Ivanova, N. 2008, ApJS, 174, 223
Bhattacharya, D., & van den Heuvel, E. P. J. 1991, Phys. Rep., 203, 1
Bildsten, L., & Deloye, C. J. 2004, ApJ, 607, L119
Cappellari, M., et al. 2006, MNRAS, 366, 1126
Dewi, J. D. M., & Tauris, T. M. 2000, A&A, 360, 1043
Di Salvo, T., et al. 2002, A&A, 386, 535
Dobrotka, A., Lasota, J.-P., & Menou, K. 2006, ApJ, 640, 288
Dubus, G., Lasota, J.-P., Hameury, J.-M., & Charles, P. 1999, MNRAS, 303, 139
Fabbiano, G. 1989, ARA&A, 27, 87
———. 2006, ARA&A, 44, 323
Fabbiano, G., et al. 2007, ApJ, submitted (arXiv:0710.5126)
Ghosh, P., & White, N. E. 2001, ApJ, 559, L97
Gilfanov, M. 2004, MNRAS, 349, 146
Hobbs, G., Lorimer, D. R., Lyne, A. G., & Kramer, M. 2005, MNRAS, 360, 974
Humphrey, P. J., & Buote, D. A. 2006, preprint (astro-ph/0612058)
Hurley, J., R., Pols, O. R., & Tout, C. A. 2000, MNRAS, 315, 543
Irwin, J. A. 2005, ApJ, 631, 511
Irwin, J. A., Athey, A. E., & Bregman, J. N. 2003, ApJ, 587, 356
Ivanova, N., & Kalogera, V. 2006, ApJ, 636, 985
Ivanova, N., Heinke, C., Rasio, F. A., Belczynski, K., & Fregeau, J. 2008, MNRAS, 386, 553
Ivanova, N., & Taam, R. E. 2003, ApJ, 599, 516
Jeltema, T. E., Canizares, C. R., Buote, D. A., & Garmire, G. P. 2003, ApJ, 585, 756
Jordán, A., et al. 2004, ApJ, 613, 279
Juett, A. M. 2005, ApJ, 621, L25
Justham, S., Rappaport, S., & Podsiadlowski, P. 2006, MNRAS, 366, 1415
Kalogera, V., & Webbink, R. F. 1998, ApJ, 493, 351
Kalogera, V., Kolb, U., & King, A. R. 1998, ApJ, 504, 967
Kim, D.-W., & Fabbiano, G. 2004, ApJ, 611, 846
Kim, D.-W., Fabbiano, G., & Trinchieri, G. 1992, ApJ, 393, 134
Kim, D.-W., et al. 2006a, ApJ, 652, 1090
Kim, E., Kim, D.-W., Fabbiano, G., Lee, M. G., Park, H. S., Geisler, D., & Dirsch, B. 2006b, ApJ, 647, 276
King, A. R. 2002, MNRAS, 335, L13
King, A. R., Kolb, U., & Burderi, L. 1996, ApJ, 464, L127
Kundu, A., Maccarone, T. J., & Zepf, S. E. 2002, ApJ, 574, L5
———. 2007, ApJ, 662, 525
Maccarone, T. J., & Coppi, P. S. 2003, A&A, 399, 1151
Menou, K., Perna, R., & Hernquist, L. 2002, ApJ, 564, L81
Miller, J. M., Fox, D. W., Di Matteo, T., Wijnands, R., Belloni, T., Pooley, D., Kouveliotou, C., & Lewin, W. H. G. 2001, ApJ, 546, 1055
Pellegrini, S., & Fabbiano, G. 1994, ApJ, 429, 105
Piro, A. L., & Bildsten, L. 2002, ApJ, 571, L103
Portegies Zwart, S. F., Dewi, J., & Maccarone, T. 2004, MNRAS, 355, 413
———. 2005, Ap&SS, 300, 247
Press, W. H., Teukolsky, S. W., Vetterling, W. T., & Flannery, B. P. 2007, Numerical Recipes: The Art of Scientific Computing (Cambridge: Cambridge Univ. Press)
Rappaport, S., Verbunt, F., & Joss, P. C. 1983, ApJ, 275, 713
Revnivtsev, M., Churazov, E., Sazonov, S., Forman, W., & Jones, C. 2007, A&A, 473, 783
Sarazin, C. L., Irwin, J. A., & Bregman, J. N. 2000, ApJ, 544, L101
Sarazin, C. L., Kundu, A., Irwin, J. A., Sivakoff, G. R., Blanton, E. L., & Randall, S. W. 2003, ApJ, 595, 743
Sivakoff, G. R., Sarazin, C. L., & Irwin, J. A. 2003, ApJ, 599, 218
Taam, R. E., Chen, X., & Swank, J. H. 1997, ApJ, 485, L83
Taam, R. E., & Sandquist, E. L. 2000, ARA&A, 38, 113
Tanaka, Y., & Shibazaki, N. 1996, ARA&A, 34, 607
Tauris, T. M., & Dewi, J. D. M. 2001, A&A, 369, 170
Tauris, T. M., & van den Heuvel, E. P. J. 2006, in Compact Stellar X-Ray Sources, ed. W. H. G. Lewin & M. van der Klis (Cambridge: Cambridge Univ. Press), 623
Terlevich, A. I., & Forbes, D. A. 2002, MNRAS, 330, 547
Tonry, J. L., Dressler, A., Blakeslee, J. P., Ajhar, E. A., Fletcher, A. B., Luppino, G. A., Metzger, M. R., & Moore, C. B. 2001, ApJ, 546, 681
Trinchieri, G., & Fabbiano, G. 1985, ApJ, 296, 447
van Paradijs, J. 1996, ApJ, 464, L139
Voss, R., & Gilfanov, M. 2007, MNRAS, 380, 1685
White, N. E., & Ghosh, P. 1998, ApJ, 504, L31
Wu, K. 2001, Publ. Astron. Soc. Australia, 18, 443